# Accepted Manuscript

A new model for predicting the grain size of electrodeposited nanocrystalline nickel coatings containing sulphur, phosphorus or boron based on typical systems

Nitin P. Wasekar, Anthony P. O'Mullane, G. Sundararajan

Please cite this article as: Nitin P. Wasekar, Anthony P. O'Mullane, G. Sundararajan , A new model for predicting the grain size of electrodeposited nanocrystalline nickel coatings containing sulphur, phosphorus or boron based on typical systems. Jeac (2018), https://doi.org/10.1016/j.jelechem.2018.11.057

# A new model for predicting the grain size of electrodeposited nanocrystalline nickel coatings containing sulphur, phosphorus or boron based on typical systems

Nitin P. Wasekar[a,b*] , Anthony P. O'Mullane [b†*], G. Sundararajan[c]

[a]*International Advanced Research Centre for Powder Metallurgy and New Materials (ARCI), Hyderabad, 500 005, India*

[b]*School of Chemistry, Physics and Mechanical Engineering, Queensland University of Technology (QUT), QLD 4001, Brisbane, Australia*

[c] *Department of Metallurgical and Materials Engineering, Indian Institute of Technology Madras (IITM), Chennai, 600 036, India*

\* Email address: nitin@arci.res.in, anthony.omullane@qut.edu.au

† ISE member

## Abstract

Controlling the grain size in electrodeposited coatings for the prevention of corrosion is highly important. To understand the relationship with grain size and electrochemical performance many experiments need to be undertaken to vary the grain size of the deposit. In the present work the (crystallite) grain size of electrodeposited Ni coatings formed in the presence of metalloids such as boron (B), sulphur (S) and phosphorus (P) was estimated from analysing mass transfer at the cathode-electrolyte interface. A mathematical model has been proposed which indicates that the grain size of the deposit is directly proportional to current efficiency and the deposition rate while being inversely proportional to the current density and metalloid (B, S, P) content in the coatings. A simple relationship is developed which is agreement with experimental data and data that is reported in the literature. The development of such a model should significantly decrease the amount of experimentation required to achieve the desired grain size in such systems (Ni, Ni-P, Ni-B coatings) obtained by electrodeposition.

*Keywords*: Electrodeposition; Grain size; Pulse electrodeposition; Ni-P; Ni-B.

## 1. Introduction

During the last two decades, electrodeposition has been proven to be an economical process to obtain virtually porosity free bulk nanocrystalline nickel (Ni) and Ni alloy coatings for corrosion and wear resistance [1-12]. These coatings are either nickel phosphorus (Ni-P) [13-16], nickel boron (Ni-B) [17-20] or Ni containing sulphur (Ni-S) [4, 5, 21-26] where each composition has individual properties as well as different applications. Electrodeposition parameters such as current density, additive (metalloid) concentration and temperature have an influence on the nanocrystalline structure of these coatings. In the final stages of electrocrystallization, after reduction, the means by which an adatom is incorporated into the crystal lattice will determine the crystal size of the deposit. Many models have been proposed to correlate these parameters with the obtained grain size through electrocrystallization [27-30]. Budevski et al [31] presented a review on electrocrystallization nucleation and growth phenomena in electrodeposited coatings. Wong et al [30] proposed a mathematical model for electrocrystallization in pulsed electrodeposition mode using different types of waveforms and found that ramp-down waveforms can be employed to obtain fine grained structures. In a similar way, Molina and Hoyos [32] estimated the hardness of pulse current deposited nickel through the indirect effect of grain size on hardness. Choo et al [28] qualitatively concluded that in order to have nanocrystalline grain sizes, during electrodeposition, a high negative over potential, high adion population and low adion surface mobility are required for a high nucleation rate and therefore reduced grain size. Rashidi and Amadeh [25] proposed a relationship between saccharin concentrations in the plating electrolyte with Ni grain size using a Langmuir type adsorption isotherm. However, this model does not give a relationship between grain size and the sulphur content in the coating. In another semi-quantitative study [8] these authors suggested that current density can lead to different grain sizes in Ni coatings depending upon the composition of the electrolyte. However, there was no direct quantification of the influence of current density on grain size. Indeed, many studies reveal conflicting data for the relationship between grain size and current density [33, 34], however, many of these proposed relationships are qualitative in nature via interpreting direct experimental observation rather than developing a physical model behind the electrodeposition process.

During electrodeposition, there are many parameters (current density, current efficiency, deposition rate, alloying/impurity content etc.) for a given pH and temperature which can be experimentally chosen. We believe for a given experiment; all these parameters have a collective effect on the grain size of a Ni coating. The main aim of the present work is therefore, to study the influence of the above mentioned parameters to quantify the grain size of electrodeposited Ni coatings containing metalloid atoms such as sulphur, phosphorus and boron and develop a phenomenological model to predict the final grain size under specific conditions. This model can also be utilized to estimate the sulphur or phosphorus or boron content of electrodeposited Ni (Ni-S, Ni-P or Ni-B) coatings if current efficiency and grain size is known. The proposed model can also be used to predict hardness of the coatings through the estimated grain size utilizing the classical Hall-Petch relation.

## 2. Results and Discussion

### A model for predicting the grain size in electrodeposited coatings

The source of metalloids such as Sulphur (S), phosphorus (P) and boron (B) used in Nickel plating baths are saccharin, phosphoric acid and borane dimethylamine respectively to generate Ni-S, Ni-P and Ni-B coatings. The S, P and B atoms or metalloids are deposited with Ni during the electrodeposition process. Since the room temperature solid solubility of these atoms is near to zero in Ni, the only space they can deposit is at the grain boundaries of Ni thereby contributing to controlling the grain size. We therefore assume that during the electrodeposition process, these atoms (metalloid) are segregated at the grain boundaries and the intercrystalline regions of the Ni grains as illustrated in Fig. 1. Since grain boundaries are defects and regarded as open space compared to a grain interior, the assumption is assumed to be valid. We also assume that these are the adsorption sites for the metalloid atoms and that the electrodeposition of Ni proceeds on the free surface i.e. at the grain interior. This is in agreement with Bockris and Reddy [35] who suggested that the single crystal electrogrowth mechanism is valid for polycrystalline growth by considering each grain as a single crystal micro substrate.

During electrodeposition, ionic species which are consumed at the electrode must be transported towards the cathode solution interface. This transport happens though a diffusion layer formed because of a concentration difference (due to the formation of a depletion layer when current is applied) near the electrode surface. This is valid as the transport number of

Ni cations is 0.02 [28], indicating that only 2 out of 100 Ni atoms are deposited by electric migration towards the cathode surface and the rest must reach the cathode surface through diffusion.

The rate of metal deposited on the electrode is equal to the rate of ions consumed at the cathode. Ibl [36] proposed a duplex diffusion layer model for pulsed electrodeposition. The schematic concentration profile near the cathode solution interface in pulsed electrodeposition is shown in reference [36].

According to Fick's law,

$$N = D\frac{dc}{dx} \tag{1}$$

where N is number of moles diffusing per unit time through a cross section of unit area i.e. flux density of mass transport (mol/cm$^2$/sec), $c$ is concentration of ionic species and $x$ is distance from cathode surface. The flux density ($N_c$) (is rate of consumption in mole/cm$^2$/sec) of cations during pulsed electrodeposition is given by,

$$N_c = D\frac{(C_0 - C_s)}{\delta_p} \tag{2}$$

where, D is the diffusion coefficient ($0.76 \times 10^{-5}$ cm$^2$/s) of Ni ions [28]. $C_s$, $C_0$ is the ionic concentration at the interface and initial concentration of ions in solution respectively, $\delta_p$ is the thickness of the pulsating diffusion layer (cm) and $N_c$ is the rate of consumption of cations (mole/cm$^2$/sec). In equation (2), the concentration difference, ($C_0$-$C_s$) is unknown which can be obtained from the Nernst diffusion model and assuming a linear concentration profile near the cathode surface. In order to have deposition of Ni ions due to an imposed current ($i_a$ - average current density, A/cm$^2$) on the surface of the cathode per unit area, an equal number of moles of cations must be removed from the stationary diffusion layer in solution. Thus according to Ibl [36],

$$\frac{C_s}{C_0} = 1 - \frac{i_a(\delta_N - \delta_p)}{C_0 nDF} \tag{3}$$

In this equation, $\delta_N$ is the Nernst diffusion layer thickness (cm), $n$, $F$ are the number of electrons (2 for Ni) and Faraday's constant (96485.33 C mol$^{-1}$) respectively.

From equations (2) and (3), the rate of consumption of metal ions from solution (mole/cm$^2$/sec) can be given by,

$$N_c = \frac{i_a(\delta_N - \delta_p)}{n.F.\delta_p} \tag{4}$$

The thickness of the pulsating diffusion layer [36] can be described by,

$$\delta_p = \sqrt{\left(2Dt_{on}\left(1 - \frac{t_{on}}{T}\right)\right)} \tag{5}$$

where, $t_{on}$ and $T$ are 'on time' and 'repetition period' (inverse of frequency) respectively in pulsed current electrodeposition. In general, $\delta_p$ is very small compared to $\delta_N$. As per Ibl [36], under most hydrodynamic conditions, $\delta_N = 10$ μm to 500 μm whereas $\delta_p = 1$ μm to 5 μm for Ni ($D = 0.76 \times 10^{-5}$ cm$^2$/s).

In addition, $\delta_N$ can also be obtained using the Levich equation,

$$\delta_N = 2.11D^{1/3}\upsilon^{1/6}\omega^{-1/2} \tag{6}$$

where, $\upsilon$ is the kinematic viscosity (cm$^2$/s) and for a Ni plating solution, $\upsilon = 1.49 \times 10^{-2}$ cm$^2$/s [28] and $\omega$ is the rotation rate (rpm). Using the kinematic viscosity of a Ni solution and the diffusion coefficient of Ni ions, 50 rpm as the rotation speed of the electrode [5], $\delta_N = 254$ μm which is within the range proposed by Ibl [36].

The rate of incorporation (mole/cm$^2$/sec) of Ni atoms in a coating can be obtained as follows. We assume that Ni deposition only happens inside grains surrounded by metalloid atoms and that the metal grain has a tetrakaidecahedron shape (actual shape of a grain/crystallite) which is a 14 sided figure having 8 regular hexagons and 6 squares. It can be created by truncating a regular octahedron. The volume of such a grain shape can be obtained as,

$$V = 8\sqrt{2}\ a^3 \tag{7}$$

The surface area therefore is,

$$S = (6 + 12\sqrt{3})\ a^2 \tag{8}$$

The distance from centre of a grain to its hexagonal side is,

$$r_6 = \sqrt{6}/2\ a \tag{9}$$

And that from square side is,

$$r_4 = \sqrt{2}\ a \tag{10}$$

Therefore,

$$\frac{V}{S} = \frac{8\sqrt{2}a^3}{6(1+2\sqrt{3})a^2} = 0.422\ a \tag{11}$$

From the hexagonal side (for grain size d),

$$\frac{V}{S} = 0.422\left(\frac{2r_6}{\sqrt{6}}\right) = 0.344r_6 = 0.172d_6 = \frac{1}{5.8}d_6 \tag{12}$$

Therefore, a metalloid e.g. sulphur $[M_{gb}]$ at a grain boundary can be given by [37],

$$[M_{gb}] = \frac{[M]}{5.8\ \delta}d_6 \tag{13}$$

Where, $M$ is the metalloid content of the coating (atomic fraction) and $\delta$ is the grain boundary thickness (~0.8 - 1 nm).

The rate of incorporation of Ni in moles/cm$^2$/sec can be given by [38, 39],

$$N_{inc} = \left(\frac{\rho}{M}\right)\eta\left(\frac{1}{[M_{gb}]}\right)t \tag{14}$$

where, $\rho$, $M$, $\eta$, $t$ are density (8.9 g/cm$^3$) and molecular weight (58.69 g/mol) of Ni, current efficiency and deposition rate (cm/s) respectively.

Upon using equation (13) and (14),

$$N_{inc} = \left(\frac{\rho}{M}\right)\eta\left(\frac{5.8\delta}{[M]\mathrm{d}}\right)t \tag{15}$$

For simplicity $d = d_6$ in equation (13)

Now as per mass balance [22],

Rate of incorporation ($N_{inc}$) = Rate of consumption ($N_c$)

Therefore, from equations (4) and (15),

$$d = \frac{\rho}{M}\cdot\eta\cdot t\cdot\frac{5.8\ \delta}{[M]N_c} \tag{16}$$

Since, $\rho/M$ = 0.152, and $\delta$ = 0.8×10$^{-7}$ cm, the final expression for the grain size of electrodeposited Ni containing metalloids such as sulphur, boron and phosphorus is given by,

$$d\ (nm) = 0.705\cdot\frac{\eta\cdot t}{[M]\cdot N_c} \tag{17}$$

Equation 17 suggests that the grain size in the presence of an insoluble metalloid in Ni is directly proportional to current efficiency and deposition rate. However, it is inversely proportional to the metalloid content (at %) of the coating and the average current density (equation 4).

The above equation gives quantitative estimation of the grain size in electrodeposited Ni coatings in the presence of metalloid such as B, S or P. Below we discuss some examples for validating this model.

**Effect of electrodeposition parameters on grain size:**

   (a) Influence of current density:

It is known that current density affects the nucleation and growth of deposits during the electrodeposition process through the applied over potential as per the Butler–Volmer equation [35]. The increase in current density increases the over potential thereby increasing the rate of nucleation. Mimani and Mayanna [40] observed that, in the presence of additives (metalloid) for a given current density the overpotential increases with an increase in concentration of metalloid. This is due to retardation of surface diffusion of the metal ions by the metalloid (e.g. Sulphur from saccharin) to the lattice at growth sites. The results presented in Fig. 2(a) predict the above phenomena. In this figure, the predicted grain size is plotted against current density at three different metalloid contents. For a given current density, an increase in the metalloid content of the coating can lead to more refined grains in electrodeposited Ni. Many other authors [21-25] presented similar results while studying the influence of current density on Ni electrodeposition.

   (b) Influence of current efficiency:

As per Faradays laws, the efficiency with which the charge is transferred in an electrochemical reaction is referred to as current efficiency. Higher current efficiency implies greater conversion of ionic species into the metallic state. This means that more metallic ions are available at growth steps thereby favouring grain growth rather than further nucleation. This is evident from Fig. 2 (b) where for a given metalloid content, deposition rate and current density, a larger grain size can be obtained with an increase in current efficiency.

(c) Influence of deposition rate:

Deposition rate (thickness/time) is related to current density and current efficiency as per Faraday's law (i.e. quantity of electrochemical reaction on an electrode is proportional to electric charge passed),

$$Deposition\ rate\ (t) = \frac{i_{avg} \cdot \eta \cdot E}{\rho} \tag{18}$$

Where, $E$ is the electrochemical equivalent of Ni (1.095 g/A.h).

As per equation (18), for a given current density, the deposition rate is proportional to the current efficiency suggesting an increased grain size with an increase in deposition rate for a given metalloid content through similar effects as mentioned above for current efficiency (Fig. 2(c)).

In fact, using equations (4), (17) and (18), it can be seen that,

$$d = \eta^2 \cdot \frac{5.8\ \delta \cdot \delta_p}{[M] \cdot (\delta_N - \delta_p)} \tag{19}$$

Since, $\frac{E}{M} \cdot \frac{nF}{3600} \approx 1$

Where $E$ = electrochemical equivalent of Ni (g/A.sec).

Since, in equation (19), other parameters are constant, the grain size is a function of only current efficiency and metalloid content in the Ni coatings. Therefore,

$$d = K \cdot \frac{\eta^2}{[M]} \tag{20}$$

Where, $K = \frac{5.8\ \delta \cdot \delta_p}{(\delta_N - \delta_p)}$

Equation (20) suggests that the grain size is a function of current efficiency and metalloid content in the Ni coatings. This is an important observation as reported in a recent study by Wasekar et al [5], where they found that the grain size of Ni coatings was independent of

current density in the presence of saccharin [5] which is a source of sulphur. If the changes in current density leads to changes in metalloid content e.g. using pulse reverse current, then it in turn leads to changes in the grain size. This suggests that it is the metalloid content (or insoluble impurities) (which might be affected by current density) that is the dominant factor for controlling the grain size at a given current efficiency.

The constant $K$ requires, $\delta_p$ and $\delta_N$ to be calculated. Unfortunately, many literature sources do not quote certain parameters (e.g. rpm) to exactly calculate the value of $\delta_N$. We assume it depends upon the electrolyte properties such as pH and composition (through kinematic viscosity). It suggests that the ratio $\delta_p/(\delta_N-\delta_p)$ is a function of particular electrolyte composition and experimental conditions. Having explained the influence of individual parameters in equation (16), the data from literature will be compared with the estimated grain size. For that purpose, we have taken data for Ni-Sulphur, Ni-boron and Ni-P system from the literature. Since most of the data in the literature is devoid of either metalloid content, current efficiency or deposition rate, the grain size data for only a few of the Ni-metalloid systems studied could be provided.

**Comparison with Literature**

Case I (Nickel-Sulphur system):

Wasekar et al [5], presented the influence of pulsed current density on the grain size of electrodeposited Ni coatings in the presence of saccharin. In this work, the sulphur content, deposition rate and current efficiency is also provided. The pH of solution was 4.5 and the operating temperature was 50°C. The data for pulsed electrodeposited Ni coatings is presented in Table 1. In this work, $t_{on}$= 20 ms and $t_{off}$ = 3 ms, as per equation 5 and equation 6, $\delta_p$ =1.99 μm and $\delta_N$ = 245 μm for the given electrolyte [5]. Therefore, the ratio of $(\delta_N-\delta_p)/\delta_p$ ≈ 127. The calculated grain size using equation 16 and equation 19 is presented in Table 1. Excellent correlation (> 98 %) can be obtained with the experimental and measured values.

Choo et al. [28] presented the influence of saccharin content on the grain size of electrodeposited Ni coatings using pulsed current deposition. In that study the experimental conditions ($t_{on}$ = 2.5 ms, $t_{off}$ = 45 ms at the peak current density 1.9 A/cm$^2$) were presented which makes it possible to calculate the diffusion layer thickness (≈ 1.89 μm). The pH of solution was maintained at 2 and the operating temperature was 65°C. The value of $\delta_N$ was

estimated to be 485 μm [41] since $\delta_N$ varies with pH, pulse conditions and hydrodynamic conditions of the solution. Choo et al. [28] utilized an unstirred solution (stagnant) during deposition which makes $\delta_N$ larger. This is due to largely varying pulses (short on time and long off time) near the cathode surface which results in a concentration change and different hydrodynamic movement due to buoyancy forces [41]. In addition, hydrogen evolution in the case of low pH solutions, changes the $\delta_N$ to large values [41, 42]. Therefore, the ratio of stationary to a pulsating diffusion layer ≈ 254. In this work the deposition rate was assumed to be $2.58\times10^{-6}$ cm/sec and according to equation 4, the consumption rate = $1.32\times10^{-4}$ moles/cm$^2$/sec. Using these values, the estimated grain size obtained as per equations 16 and 20 are presented in Table 2. The obtained grain size is within 10% of the reported value.

The data from several sources in the literature was also compared with the present model as presented in Fig.3. For that purpose, the Ni grain size was calculated considering a sulphur content of 0.16 at%, deposition rate of $2.5\times10^{-6}$ cm/sec at a current efficiency of 99 %. The calculated grain size data with current density is plotted along with the reported literature. The literature data was found to follow the predicted trend.

It can be observed that in the presence of S containing additives, the grain size becomes independent of current density above 0.1 A/cm$^2$. The grain size remains constant in the range of 18-21 nm. This is due to saturation of adsorption sites as observed by other investigators [4, 5, 24] through diffusional process which controls inhibition, consumption as well as incorporation of S in the coating. In fact, the S content of the coating follows a Langmuir adsorption isotherm (i.e. relation between saccharin content in the electrolyte and the S content of the coating) [22]. This implies that the S content reaches a saturation limit above a certain concentration which happens at a particular current density. In order to find out this critical current density, the following example was explored.

Choo et al. [28] reported the influence of saccharin concentration on the S content of Ni coatings. It was observed that the saturation of S content in the coating happens at 5 g/l of saccharin in the electrolyte. The corresponding S content of the coating is 0.0864 at%. With this S content and constant grain size ≈20 nm, using equation 16, the critical current density for saturation of the grain size is 0.12 A/cm$^2$ which is similar to the current density in Fig. 3. Thus for the Ni-S system, above this current density, there will not be any further changes in the grain size due to saturation of adsorption sites with sulphur [5].

Case II (Nickel-Boron system):

According to the Ni-B phase diagram, the solid solubility of B in Ni is nil at room temperature as well as at typical electrodeposition process temperatures and therefore it forms a super saturated solid solution similar to nickel-phosphorus. Hence in line with the Ni-S system as mentioned before, we have calculated the grain size as per equation 19 since the data for the deposition rate is not available. In this case we have assumed a current efficiency of 98 % and the ratio of $(\delta_N-\delta_p)/\delta_p \approx 127$ similar to the Ni-S system. The calculated grain size as a function of B content was then plotted along with the grain size reported in the literature as shown in Fig. 4 where excellent correlation with the reported values is evident. This suggests that the model is also applicable to the electrodeposited Ni-B system.

Case III (Nickel-Phosphorus system):

In this system, the calculated grain size as per equation 19 is plotted against phosphorus content of Ni-P coatings obtained from literature data. The average current efficiency is assumed to be ~41% since it is very well known that the P content of solution affects the current efficiency [46]. The constant, $(\delta_N-\delta_p)/\delta_p \approx 1.27$ was estimated from the pulse parameters of Chen et al. [48] with kinematic viscosity = 0.0123 cm$^2$/sec [49], $D = 0.65\times10^{-5}$ cm$^2$/sec [49] for Ni-P solution resulting in $\delta_N = 13.45$ μm and $\delta_p = 5.92$ μm. The constant $(\delta_N-\delta_p)/\delta_p \approx 1.27$ which is very small compared to the previous cases of 127 which may be due to the fact that the hydrodynamic conditions must be affected by the P bearing molecule by changing the viscosity and pH of the solution which is an aspect that needs further study. However, the estimated grain size from equation 19 was 15.4 nm which is close to the work of Chen [48] who reported a value of 14.8 nm. The plot in Fig. 5 suggests that the model fits well with experimentally reported values from the literature.

## 3. Conclusions

A phenomenological model which correlates experimentally obtained parameters such as current efficiency and metalloid content with the grain size of electrodeposited Ni coatings is

proposed provided that the metalloid has no solid solubility at room temperature with Ni. It was predicted that the grain size of electrodeposited Ni containing boron, sulphur, phosphorus is directly proportional to the current efficiency, deposition rate and is inversely proportional to metalloid content and current density. In essence, the model can also be used to estimate the sulphur, phosphorus and boron content of corrosion protection coatings if other parameters are known as per equation 17. In addition, the present study could in principle be extended to other systems such as Cu, Fe, Co, Au, Ag, Rh and other metals that can be electrodeposited in the presence of sulphur, phosphorus or boron containing additives/chemicals and where there is a limitation on room temperature solid solubility in an alloy leading to grain boundary segregation at room temperature.

## Acknowledgement

## References

1. I. Gurrappa, L. Binder, Electrodeposition of nanostructured coatings and their characterization—a review, Sci. Technol. Adv. Mater., 9 (2008) 043001.

2. G. Devaraj, S. Guruviah, S.K. Seshadri, Pulse plating, Mater. Chem. Phys., 25 (1990) 439-461.

3. U. Erb, A.M. El-Sherik, G. Palumbo, K.T. Aust, Synthesis, structure and properties of electroplated nanocrystalline materials, Nanostructured Mater., 2 (1993) 383-390.

4. A.M. El-Sherik, U. Erb, Synthesis of bulk nanocrystalline Nickel by pulsed electrodeposition, J. Mater. Sci., 30 (1995) 5743-5749.

5. N.P. Wasekar, P. Haridoss, S.K. Seshadri, G. Sundararajan, Influence of mode of electrodeposition, current density and saccharin on the microstructure and hardness of electrodeposited nanocrystalline nickel coatings, Surface Coatings Technol., 291 (2016) 130-140.

6. N.P. Wasekar, P. Haridoss, S.K. Seshadri, G. Sundararajan, Sliding wear behavior of nanocrystalline Nickel coatings: Influence of grain size, Wear, 296 (2012) 536-546.

7. A.M. Pillai, A. Rajendra, A.K. Sharma, Pulse electrodeposition of nanocrystalline nickel on AA 6061 for space applications, Transactions of the IMF, 90 (2012) 44-51.

8. A.M. Rashidi, A. Amadeh, The effect of current density on the grain size of electrodeposited nanocrystalline Nickel coatings, Surface and Coatings Technol., 202 (2008) 3772-3776.

9. H. Natter, R. Hempelmann, Tailor-made nanomaterials designed by electrochemical methods, Electrochim. Acta, 49 (2003) 51-61.

10. C. Ma, S.C. Wang, F.C. Walsh, Electrodeposition of nanocrystalline nickel and cobalt coatings, Transactions of the IMF, 93 (2015) 8-17.

11. D.H. Jeong, U. Erb, K.T. Aust, G. Palumbo, The relationship between hardness and abrasive wear resistance of electrodeposited nanocrystalline Ni–P coatings, Scripta Materialia, 48 (2003) 1067-1072.

12. S.H. Kim, U. Erb, K.T. Aust, F. Gonzalez, G. Palumbo, The corrosion behavior of nanocrystalline electrodeposits, Plating and Surface finishing, 91 (2004) 68-70.

13. G. McMahon, U. Erb, Structural transitions in electroplated Ni-P alloys, J. Mater. Sci. Lett., 8 (1989) 865-868.

14. L. Chang, C.H. Chen, H. Fang, Electrodeposition of Ni–P Alloys from a sulfamate electrolyte relationship between bath pH and structural characteristics, J. Electrochem. Soc., 155 (2008) D57-D61.

15. E. Bredael, B. Blanpain, J.-P. Celis, J.R. Roos, On the amorphous and crystalline state of electrodeposited Nickel-Phosphorus coatings, J. Electrochem. Soc., 141 (1994) 294-299.

16. M. Yan, H.G. Ying, T.Y. Ma, Improved microhardness and wear resistance of the as-deposited electroless Ni–P coating, Surface and Coatings Technol., 202 (2008) 5909-5913.

17. Y.N. Bekish, S.K. Poznyak, L.S. Tsybulskaya, T.V. Gaevskaya, Electrodeposited Ni–B alloy coatings: structure, corrosion resistance and mechanical properties, Electrochim. Acta, 55 (2010) 2223-2231.

18. C.-R. Chang, K.-H. Hou, M.-D. Ger, J.-R. Wang, Characteristics of Nickel Boron coatings prepared by direct current electrodeposition technique, Int. J. Electrochem. Sci., 12 (2017) 2055-2069.

19. J.R. López, P.F. Méndez, J.J. Pérez-Bueno, G. Trejo, G. Stremsdoerfer, Y. Meas, The effect of boron content, crystal structure, crystal size on the hardness and the corrosion resistance of electrodeposited Ni-B coatings, Int. J. Electrochem. Sci, 11 (2016) 4231-4244.

20. K.H. Lee, D. Chang, S.C. Kwon, Properties of electrodeposited nanocrystalline Ni–B alloy films, Electrochim. Acta, 50 (2005) 4538-4543.

21. M. Bhardwaj, K. Balani, R. Balasubramaniam, S. Pandey, A. Agarwal, Effect of current density and grain refining agents on pulsed electrodeposition of nanocrystalline nickel, Surf. Eng., 27 (2011) 642-648.

22. J. Edwards, Aspects of addition agent behaviour, Transactions of the IMF, 41 (1964) 169-181.

23. E. Moti, M.H. Shariat, M.E. Bahrololoom, Electrodeposition of nanocrystalline nickel by using rotating cylindrical electrodes, Mater. Chem. Phys., 111 (2008) 469-474.

24. Y. Nakamura, N. Kaneko, M. Watanabe, H. Nezu, Effects of saccharin and aliphatic alcohols on the electrocrystallization of nickel, J. Appl. Electrochem., 24 (1994) 227-232.

25. A.M. Rashidi, A. Amadeh, The effect of saccharin addition and bath temperature on the grain size of nanocrystalline nickel coatings, Surface and Coatings Technol., 204 (2009) 353-358.

26. F. Yang, W. Tian, H. Nakano, H. Tsuji, S. Oue, H. Fukushima, Effect of current density and organic additives on the texture and hardness of Ni electrodeposited from sulfamate and Watt's solutions, Mater. Trans., 51 (2010) 948-956.

27. D.T. Chin, Mass transfer and current-potential relation in pulse electrolysis, J. Electrochem. Soc., 130 (1983) 1657-1667.

28. R.T.C. Choo, J.M. Toguri, A.M. El-Sherik, U. Erb, Mass transfer and electrocrystallization analyses of nanocrystalline nickel production by pulse plating, J. Appl. Electrochem., 25 (1995) 384-403.

29. D. Grujicic, B. Pesic, Electrodeposition of copper: the nucleation mechanisms, Electrochim. Acta, 47 (2002) 2901-2912.

30. K.P. Wong, K.C. Chan, T.M. Yue, Modeling of electrocrystallization for pulse current electroforming of nickel, Appl. Surf. Sci., 178 (2001) 178-189.

31. E. Budevski, G. Staikov, W.J. Lorenz, Electrocrystallization: nucleation and growth phenomena, Electrochim. Acta, 45 (2000) 2559-2574.

32. J. Molina, B.A. Hoyos, Modeling of grain size and hardness for pulse current electroplating, Electrochim. Acta, 54 (2009) 1784-1790.

33. F. Ebrahimi, Z. Ahmed, The effect of current density on properties of electrodeposited nanocrystalline nickel, J. Appl. Electrochem., 33 (2003) 733-739.

34. A. Cziraki, B. Fogarassy, I. Geröcs, E. Toth-Kadar, I. Bakonyi, Microstructure and growth of electrodeposited nanocrystalline nickel foils, J. Mater. Sci., 29 (1994) 4771-4777.

35. J.O.M. Bockris, A.K.N. Reddy, Modern Electrochemistry, Plenum Press, New York, 1970.

36. N. Ibl, Some theoretical aspects of pulse electrolysis, Surface Technol., 10 (1980) 81-104.

37. G.D. Hibbard, K.T. Aust, U. Erb, The effect of starting nanostructure on the thermal stability of electrodeposited nanocrystalline Co, Acta Materialia, 54 (2006) 2501-2510.

38. M.S. Abrahams, S.T. Rao, C.J. Buiocchi, L. Trager, Decorated boundaries observed in copper electrodeposits, J. Electrochem. Soc., 133 (1986) 1786-1791.

39. L. Beaunier, M. Froment, C. Vignaud, A kinetical model for the electrochemical grooving of grain boundaries, Electrochim. Acta, 25 (1980) 1239-1246.

40. T. Mimani, S. Mayanna, Thermodynamics of adsorption of brighteners on polarized nickel from Watts bath solution, J. Electrochem. Soc., 140 (1993) 984-988.

41. O. Kardos, Current distribution on microprofiles, Plating, 61 (1974) 129.

42. A. Nishikata, Y. Ichihara, Y. Hayashi, T. Tsuru, Influence of electrolyte layer thickness and pH on the initial stage of the atmospheric corrosion of iron, J. Electrochem. Soc., 144 (1997) 1244-1252.

43. L. Wang, Y. Gao, T. Xu, Q. Xue, A comparative study on the tribological behavior of nanocrystalline nickel and cobalt coatings correlated with grain size and phase structure, Mater. Chem. Phys., 99 (2006) 96-103.

44. D. Pin-Qiang, Y. Hui, L. Qiang, Trans. Mater. Heat Treatment, 25 (2004) 1283-1286.

45. J.-X. Kang, W.-Z. Zhao, G.-F. Zhang, Influence of electrodeposition parameters on the deposition rate and microhardness of nanocrystalline Ni coatings, Surface and Coatings Technol., 203 (2009) 1815-1818.

46. A. Ordine, S. Diaz, I. Margarit, O. Barcia, O. Mattos, Electrochemical study on Ni–P electrodeposition, Electrochim. Acta, 51 (2006) 1480-1486.

47. M. Yan, H.G. Ying, T.Y. Ma, Improved microhardness and wear resistance of the as-deposited electroless Ni–P coating, Surface and Coatings Technol., 202 (2008) 5909-5913.

48. F.J. Chen, Y.N. Pan, C.Y. Lee, C.S. Lin, Internal stress control of nickel–phosphorus electrodeposits using pulse currents, J. Electrochem. Soc., 157(3) (2010) D154-D158.

49. S. Chen, K.M. Yin, R.E. White, A mathematical model for the electrodeposition of alloys on a rotating disk electrode, J. Electrochem. Soc., 135(9) (1988) 2193-2200.

Table 1. Calculated grain size for Nickel Sulphur system as per data presented in reference [5].

| Average Current Density (A/cm$^2$) | Sulphur content (at %) | Current efficiency η | Deposition rate, $t$ (cm/sec) | Consumption rate, $N_c$ (Equation 4) | Grain size (nm) (Equation 16) | Grain size (nm) (Equation 19) | Experimental/ Reported grain size (nm) |
|---|---|---|---|---|---|---|---|
| 0.08696 | 0.11980 | 0.87 | 2.59E-06 | 5.68E-05 | 23.41511 | 23.17762 | 20 |
| 0.08043 | 0.11541 | 0.94 | 2.58E-06 | 5.25E-05 | 28.15978 | 27.85689 | 22 |
| 0.07391 | 0.08705 | 0.97 | 2.45E-06 | 4.83E-05 | 39.79690 | 39.37243 | 32 |
| 0.06739 | 0.07753 | 0.96 | 2.21E-06 | 4.40E-05 | 44.02492 | 43.55237 | 43 |
| 0.06087 | 0.07166 | 0.98 | 2.04E-06 | 3.97E-05 | 49.66185 | 49.13041 | 59 |
| 0.05435 | 0.06325 | 0.97 | 1.80E-06 | 3.55E-05 | 54.92587 | 54.34439 | 67 |
| 0.04783 | 0.03546 | 0.97 | 1.58E-06 | 3.12E-05 | 97.60653 | 96.57474 | 95 |
| 0.04130 | 0.01829 | 0.98 | 1.40E-06 | 2.70E-05 | 197.4231 | 193.7097 | 195 |

Table 2. Calculated grain size for Nickel Sulphur system as per data presented in reference [28].

| Average Current Density $(A/cm^2)$ | Sulphur content (at %) | Current efficiency* *[23] η | Deposition rate, $t$ (cm/sec) | Consumption rate, $N_c$ (Equation 4) | Grain size (nm) (Equation 16) | Grain size (nm) (Equation 19) | Experimental/ Reported grain size (nm) |
|---|---|---|---|---|---|---|---|
| 0.1 | 0.0408 | 0.95 | 2.58E-06 | 1.32E-04 | 32 | 40 | 45±5 |
| 0.1 | 0.0653 | 0.88 | 2.58E-06 | 1.32E-04 | 19 | 22 | 20±2 |
| 0.1 | 0.0864 | 0.87 | 2.58E-06 | 1.32E-04 | 14 | 15 | 11±1 |
| 0.1 | 0.0931 | 0.85 | 2.58E-06 | 1.32E-04 | 13 | 14 | 11±1 |
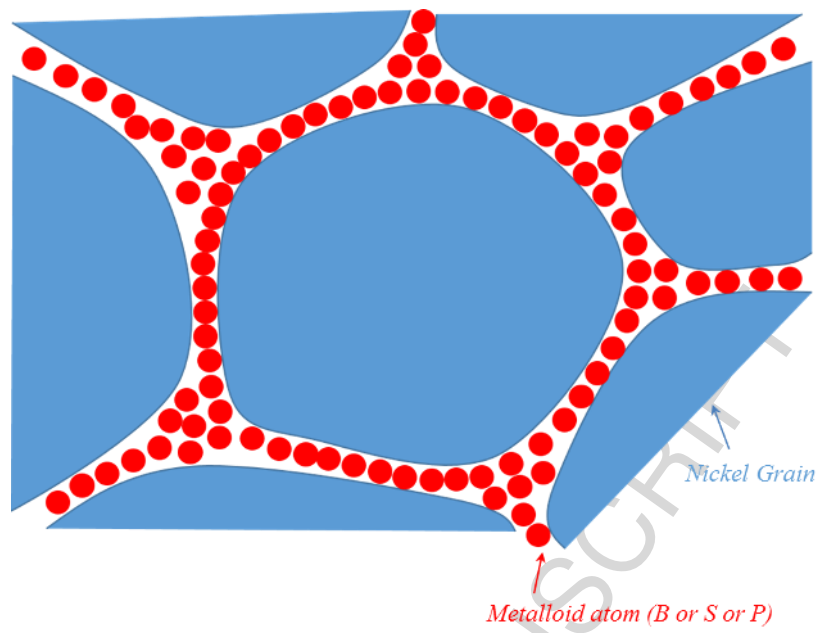
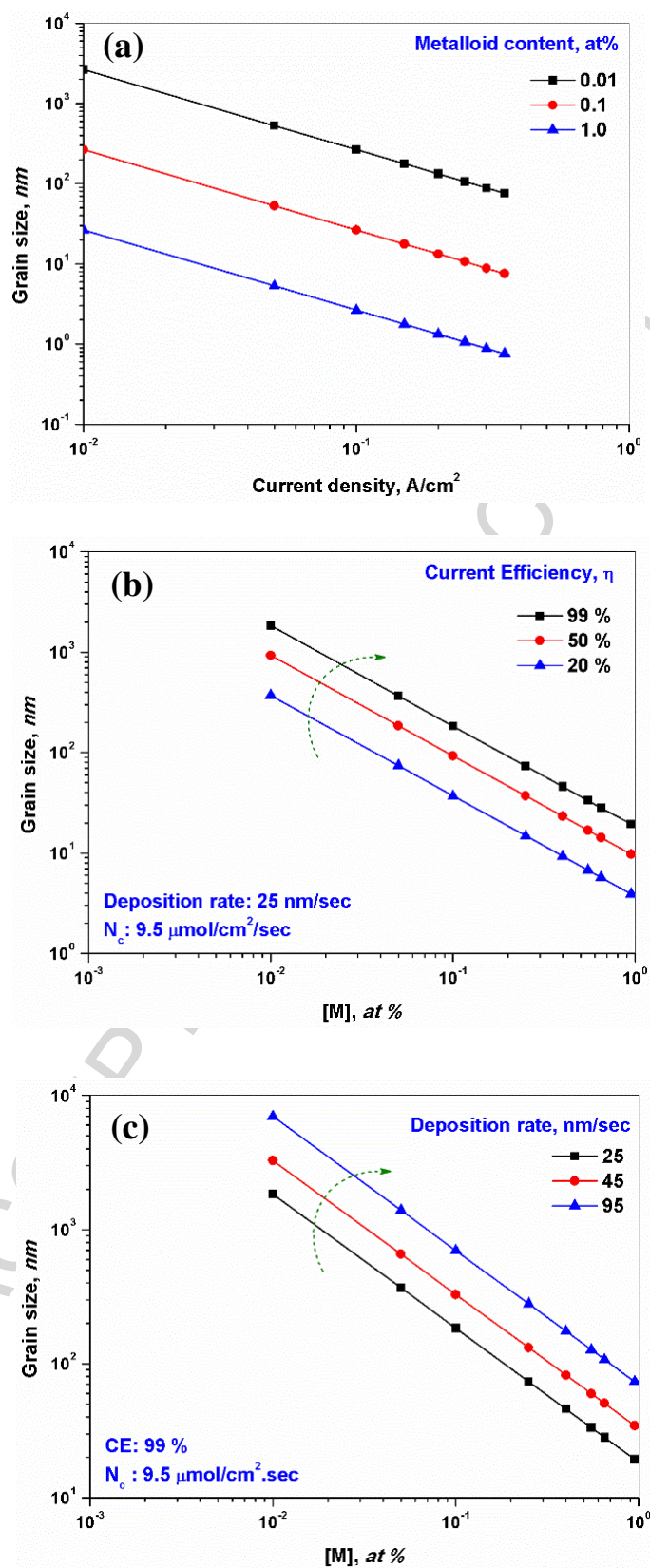Figure 1. Distribution of metalloid atoms at Ni grain boundaries (Schematic).

Figure 2. Influence of current density, current efficient and deposition rate on grain size of Ni coatings as per equation 16.
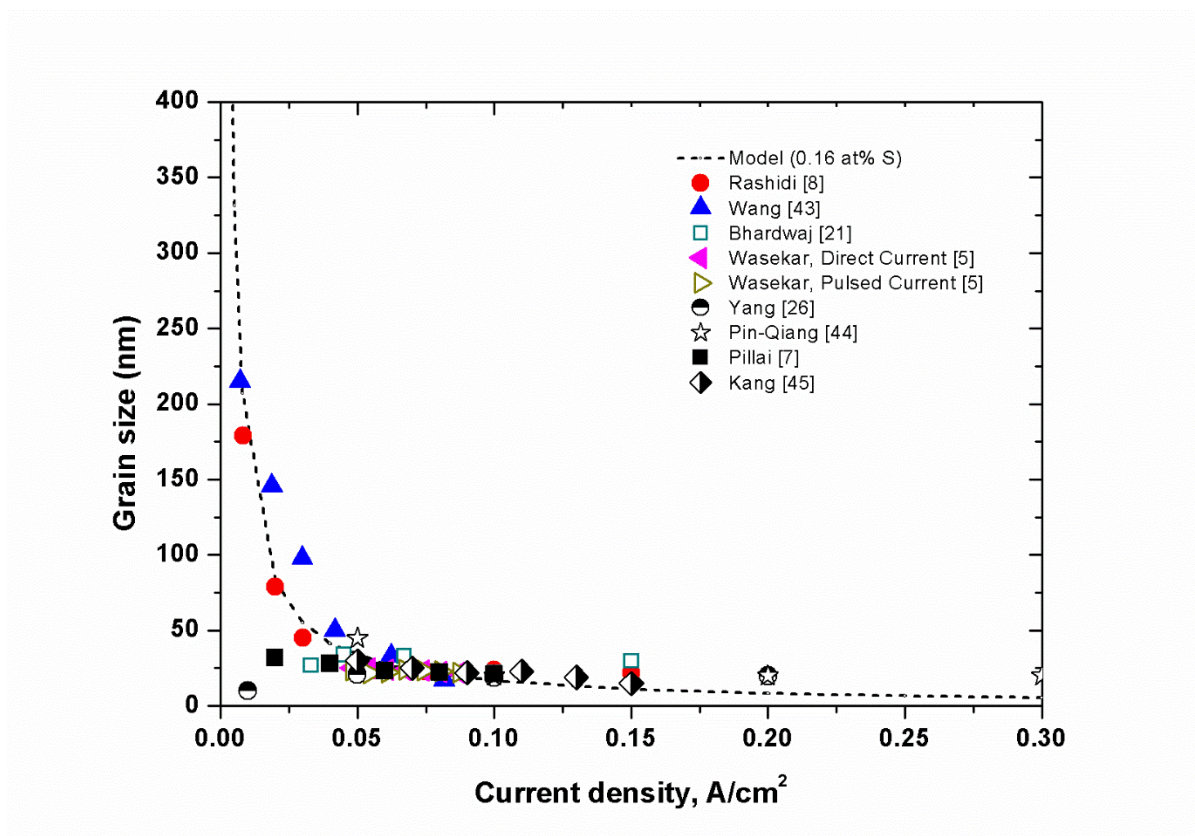
Figure 3. The literature and predicted values of grain size of Ni coatings in presence of sulphur containing additives as a function of current density.
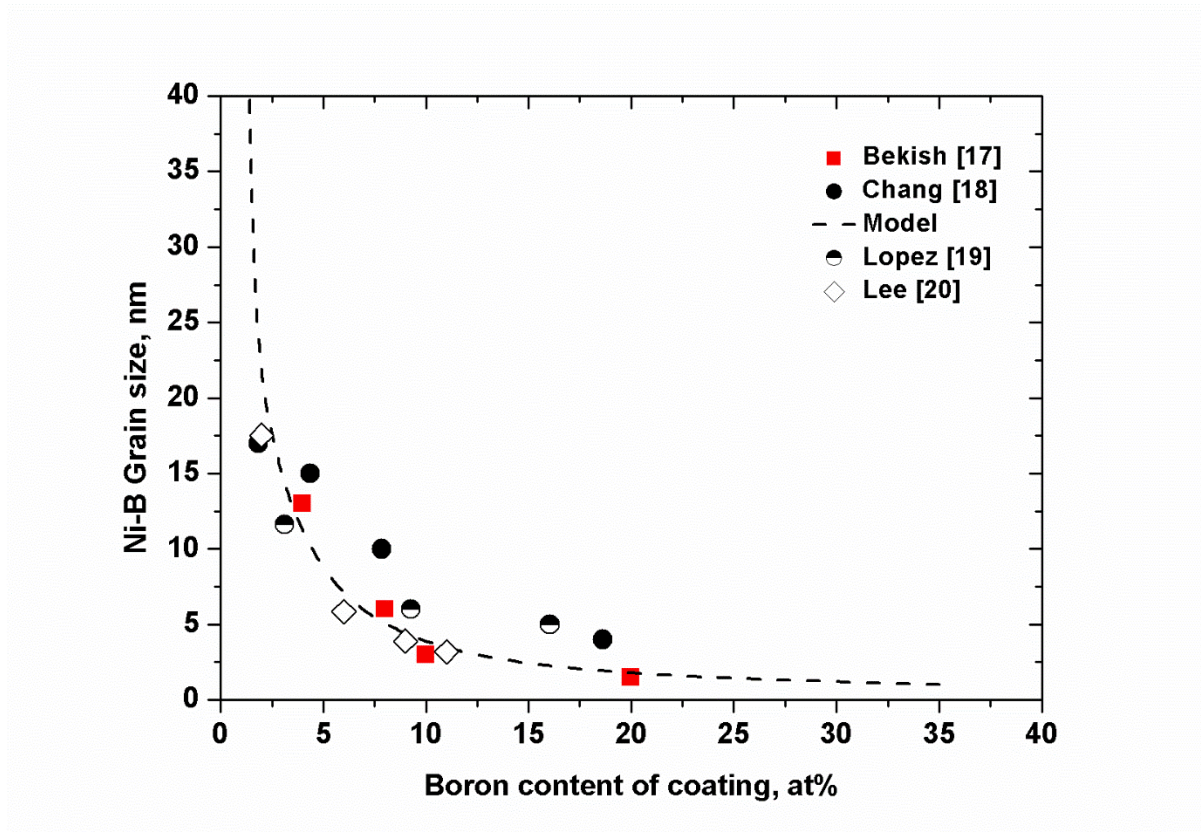
Figure 4. The literature and predicted values of grain size of Ni-B coatings as a function of current density.
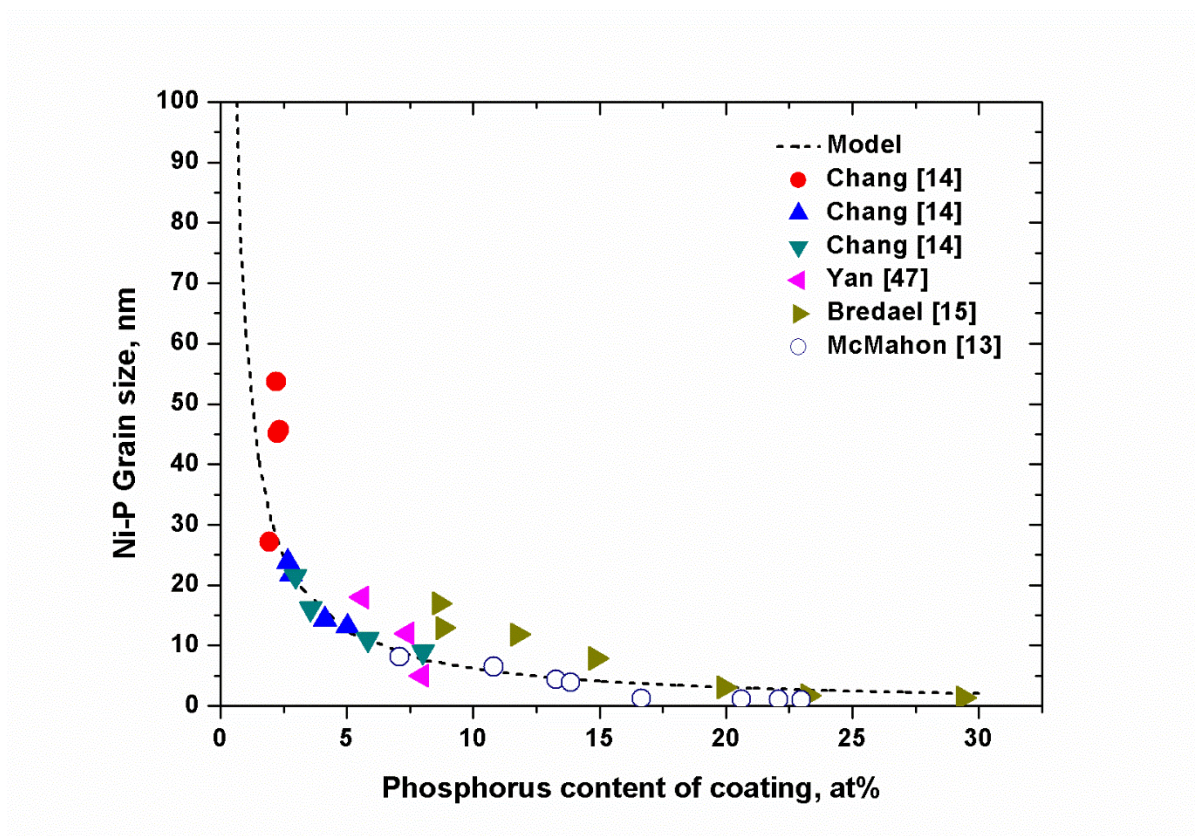
Figure 5. The literature and predicted values of grain size of Ni-P coatings as a function of current density.

**Highlights**

Model is developed for Ni-S, Ni-B and Ni-P protective coatings

Understanding the influence of metalloid content in Ni coatings for corrosion protection

Model correlating applied electrochemical deposition parameters to the grain size of the deposit